analytical chemistry

Article

Cite This: *Anal. Chem.* 2019, 91, 6051−6056

pubs.acs.org/ac

Matrix-Assisted Laser Desorption Ionization Imaging and Laser Ablation Sampling for Analysis of Fungicide Distribution in Apples

Igor Pereira,[†,‡] Bijay Banstola,[†] Kelin Wang,[†] Fabrizio Donnarumma,[†] Boniek G. Vaz,*[,‡] and Kermit K. Murray*[,†]

[†]Department of Chemistry, Louisiana State University, Baton Rouge, Louisiana 70803, United States

[‡]Chemistry Institute, Federal University of Goiás, Goiânia, Goiás, 74690-900, Brazil

Supporting Information

ABSTRACT: A combination of matrix-assisted laser desorption ionization (MALDI) imaging and infrared (IR) laser ablation sampling with offline electrospray ionization mass spectrometry (ESI-MS) was used to determine the distribution of the fungicide imazalil in apples. MALDI images were used to determine the penetration depth of imazalil up to 7 days after its application. IR laser ablation sampling and ESI-MS were used to quantify the rate of penetration of the fungicide, which was determined to be approximately 1 mm per day. Imazalil concentration decreased in the apple skin over the course of the experiment, and after 7 days the fungicide was detected at 0.015 ppm 6 mm inside the apple. Approximately 60% of the pesticide remained in the skin after 7 days. This work demonstrates the utility of MALDI imaging for spatial localization of fungicide in fruit in combination with IR laser ablation and ESI-MS for quantitative analysis.

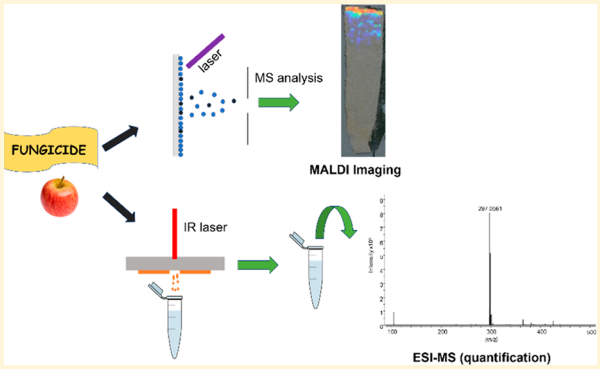

Pesticides are widely used on fruits and vegetables to avoid damage by pests or fungi in different stages of cultivation or for postharvest storage.[1] Pesticides help to ensure long storage lifetime and high product yield, but these compounds need to be applied efficiently in the lowest possible concentration to minimize environmental impact and human exposure.[2−4] Application of pesticides can be a problem if the pesticide residue adheres to the product at a concentration above the allowable limit.[5] Additionally, some pesticides can penetrate the exterior of fruits and vegetables, making ordinary peel washing an ineffective approach.[6,7] Because pesticides are designed to be toxic for living organisms, their toxicity to humans is often significant,[8] necessitating the development of advanced methods for analyzing these compounds at trace levels.

One of the most common uses of pesticides in fruits is fungicide.[9] Imazalil (1-{2-(2,4-dichlorophenyl)-2-[(prop-2-en-1-yl)oxy]ethyl}-1H-imidazole) is a postharvest fungicide that is widely used to prevents fruit degradation by controlling growth and sporulation of fungal strains.[10] The mode of action consists in inhibiting the biosynthesis of ergosterol, an essential component in the membrane of fungal cells.[11] Imazalil is efficient for the control of fungi of the *Penicillium* genus, such as *P. digitatum* and *P. italicum* in citrus fruits,[12] and *P. expansum* in pome fruits.[13] Usually, imazalil is applied to fruits after harvest by dipping, drenching, or spraying using concentrations between 1000 and 2000 ppm.[14−16] Concerns about the toxicity of imazalil derive from its potential effects on reproductive and neurobehavioral parameters[17] as well as possible genotoxic and teratogenic effects.[18] Of particular concern is whether imazalil can diffuse into the fruit after its application. The rate of diffusion can be influenced by the high polarity of imazalil which promotes transport to the high water-content interior of the fruit.[19]

Traditionally, pesticide residue determination in fruits and vegetables has been performed using gas chromatography coupled to mass spectrometry (GC−MS)[20−23] and liquid chromatography coupled to mass spectrometry (LC−MS).[24−27] Both techniques demonstrate excellent analytical performance but provide limited information on the distribution of pesticides in the sample.

Matrix-assisted laser desorption ionization (MALDI) imaging is a powerful technique for MS that allows the visualization of the localization of molecules within biological tissue.[28−32] Most MALDI imaging applications have been in analysis of animal tissue; however, there have also been a number of applications of MALDI imaging to plant tissue and to monitor the spatial localization of pesticide residue on food plants.[33−36] For example, Annangudi et al. verified the spatial distribution of the fungicides epoxiconazole, azoxystrobin, and pyraclostrobin on wheat leaf surfaces.[37] Anderson et al. monitored the translocation of four sulfonylurea herbicides, chlorimuron

Received: January 31, 2019
Accepted: April 10, 2019
Published: April 10, 2019

DOI: 10.1021/acs.analchem.9b00566
Anal. Chem. 2019, 91, 6051−6056

ethyl, chlorsulfuron, imazosulfuron, and pyrazosulfuron-ethyl, in sunflower plants 24 h after foliar application.[38] Also, Mullen et al. imaged the herbicide mesotrione and the fungicide azoxystrobin on the surface of soya leaf and azoxystrobin inside the stem of the soya plant.[39]

In addition to MALDI, an ultraviolet (UV) or infrared (IR) laser at ambient conditions can be used with online MS for localization of analytes inside biological tissues.[40,41] The laser beam is directed at a specific area of the tissue to ablate a wide range of molecular species which can be directly ionized or captured in solvent for subsequent ionization.[42] For example, IR laser ablation into an ESI source was used for single cell analysis from *Allium cepa* and *Narcissus pseudonarcissus* bulb epidermis as well as from single eggs of *Lytechinus pictus*.[43] IR laser ablation and solvent capture by aspiration with online ESI has also been used for imaging pigments in *Alstroemeria* flower petals and in red radish taproot (*Raphanus sativus* L.).[44]

Laser microdissection can be used to obtain quantitative information about plant tissue.[45] When the sample is captured, the analyte can be extracted and resuspended in an adequate volume of solvent which can result in a more concentrated analyte solution for offline MS quantitative analysis. For example, laser microdissection was used to remove pieces of the floral parts of *Cannabis sativa* plants for quantification of cannabinoids by offline LC−MS.[46] The alkaloid contents of *Sinomenii caulis* were quantified after laser microdissection and offline LC−MS.[47]

Laser ablation is an alternative to laser microdissection and is a versatile method for the capture of biomolecules from animal tissue.[48−52] Infrared laser ablation capture with offline analysis has been used to identify and quantify proteins,[53] determine the activity of captured enzymes,[54] and sample large double stranded DNA.[55] IR laser ablation is efficient at breaking up tissue and therefore the extraction of the captured material is significantly faster and more efficient compared to laser microdissection.

In this work, MALDI imaging was combined with laser ablation sampling and offline ESI-MS for the analysis of the distribution of imazalil in apples. Imazalil was applied in fresh organic Fuji apples, and the fruits were sampled on different days. The penetration of the fungicide from the peel to inner region of the fruit was monitored with MALDI imaging using apple sections, and quantification was performed on laser ablated extracts using ESI-MS. The experiment was designed for 7 days of apple storage after imazalil application to simulate rapid postharvest fungicide treatment and transport or point of sale application.

EXPERIMENTAL SECTION

Chemicals and Materials. HPLC grade acetonitrile (ACN), formic acid (FA), and trifluoroacetic acid (TFA) were purchased from Thermo-Fisher Scientific (Waltham, MA), and α-cyano-4-hydroxycinnamic acid (CHCA) was purchased from Sigma-Aldrich (St. Louis, MO). Ultrapure water (18 MΩ cm) was produced in-house. Plain glass microscope slides were purchased from Thermo-Fisher Scientific, and indium tin oxide (ITO) microscope slides were purchased from Bruker Daltonics (Bremen, Germany). Imazalil (see the structure and physicochemical properties in Figure S-1, Supporting Information) was purchased from MedChem Express (Monmouth Junction, NJ). Fresh organic Fuji apples were purchased from a local supermarket.

Sample Preparation. For all experiments, the concentration of imazalil is indicated in ppm (mg/L for solutions and mg/kg for mass of analyte in mass of apple). For MALDI imaging experiments, 12 apples were submerged for 2 min in a 4 L glass beaker containing 2 L of a 1000 ppm aqueous solution of imazalil. A control group of 4 apples was not treated. The apples were stored at room temperature for up to 7 days, which has been used previously to simulate typical application and marketing conditions.[56,57] At days 0, 1, 4 and 7, four apples (three containing imazalil and one control) were taken and 0.2 mm thick sections (one slice for each apple) were produced using a vibratome (Vibratome 1500, Ted Pella, Redding, CA) and mounted on ITO glass slides. The apples were cut perpendicular to the endocarp axis to obtain sections with the endocarp on one end and the skin on the other. The apple sections were dried under vacuum for 15 min before matrix application. For laser ablation sampling, the same approach was employed but plain glass slides were used and samples were processed without prior drying.

MALDI Imaging. A 10 mg/mL solution of CHCA in 1:1 H_2O/ACN containing 0.1% TFA was sprayed on the slides using a home-built pneumatic nebulizer with a liquid flow rate of 100 μL/min and a nitrogen gas pressure of 70 kPa (10 psig). The matrix was sprayed at a distance of 8 cm from the apple section, and 14 spray cycles of 20 s each were used. The matrix was allowed to dry for 1 min between each spray cycle. MALDI mass spectra were recorded using a tandem time-of-flight mass spectrometer (UltrafleXtreme, Bruker, Bremen, Germany). The instrument is equipped with a 355 nm Nd:YAG laser operating at a repetition rate of 1 kHz. The section surface was irradiated with 1000 laser shots and a step size of 200 μm in positive ion reflectron mode. After data acquisition, images were reconstructed using FlexImaging software (Bruker). The intensity of protonated imazalil (m/z 297.06) was used to create images.

Laser Ablation Sampling. The mid-IR laser ablation system has been described previously.[49,58] Briefly, microscope slides with samples were mounted on a two-axis translation stage (LTA-HS, Newport, Irvine, CA) operated using 50 mm actuators (LTA-HS, Newport) and a motion controller (XPS-Q8, Newport). Sample slides were irradiated in transmission geometry with a pulsed IR optical parametric oscillator (IR Opolette 2940, OPOTEK, Carlsbad, CA). The laser pulse width was 5 ns, the repetition rate was 20 Hz, and the wavelength was 2.94 μm. The beam was directed at the sample target at a 90° angle and was focused with a 50 mm focal length lens to a spot size of 200 μm × 250 μm, as measured with laser burn paper. The laser energy was set to 2.2 mJ, which corresponds to a fluence of 44 kJ/m^2. Areas of 1 mm^2 from the apple section were ablated from the skin to the endocarp. A 300 μL microcentrifuge tube with 200 μL of ACN was mounted below the microscope slide, keeping the surface of the solvent ∼5 mm from the slide. After vortexing (10 s) and centrifugation (1 min), the supernatant was collected in a new tube and dried under vacuum at room temperature. The samples were resuspended in 30 μL of ACN with 0.1% FA before ESI-MS analysis. Samples for calibration curves (Figure S-2) were prepared as described above by ablating apples that did not contain imazalil and resuspending the captured material in 30 μL of imazalil solution in ACN with 0.1% FA (concentrations of 0, 0.005, 0.01, 0.05, 0.1, 0.5, 1, and 3 ppm). The resulting solutions were injected into the ESI source for quantification analysis.

DOI: 10.1021/acs.analchem.9b00566
Anal. Chem. 2019, 91, 6051−6056

An overall extraction experiment was performed to evaluate the total sampling efficiency of the process between laser ablation and ESI-MS. The experiment was conducted by spiking 0.2 μL of three known imazalil concentrations (25, 500, and 5000 ppm) on 1 mm^2 areas of the apple sections, resulting in total deposited amounts of 0.005, 0.1, and 1 ppm, respectively. To avoid the diffusion of imazalil from the area to which it was applied, 1 mm^2 islands of apple tissue were created by ablating regions around the selected areas. Each area was separated from the adjacent areas by 1 mm. When the imazalil solution was applied to the tissue island, the droplet adhered to the tissue as the solvent evaporated to leave the imazalil confined to the 1 mm^2 region. Sample capture and preparation for ESI-MS analysis were performed as indicated above, and the signal intensity of protonated imazalil peak was compared with the signal intensity of a control (solution of imazalil in ACN). The transfer efficiency was obtained from the ratio of the imazalil signal intensity of the recovered material to that of the control.

ESI-MS. Electrospray ionization mass spectra were recorded using an Agilent 6230 TOF-MS instrument (Agilent Technologies, Santa Clara, CA). The intensity of the protonated imazalil (m/z 297.0561 [M + H]$^+$) was used for all analyses. Because the mass spectrometer does not have MS/MS capabilities, the identification of the protonated imazalil ion was based on the exact mass measurements and the isotopic cluster peaks at m/z 297, 299, and 301, which are consistent with the presence of the two chlorine atoms in the imazalil structure. The following parameters were used: capillary voltage, 4000 V; gas temperature, 325 °C; sheath gas temperature, 375 °C; drying gas flow, 10 L/min; sheath gas flow, 11 L/min; nebulizer, 35 psig; injection volume, 1 μL. The data were processed using the Agilent MassHunter Qualitative Analysis B.07.00 software.

RESULTS AND DISCUSSION

An initial experiment was performed to determine whether the signal from protonated imazalil can be used for MALDI imaging. Figure 1 shows a MALDI spectrum obtained after spiking 1 μL of a 1000 ppm imazalil solution (in ACN) with 1.4 μL of a 10 mg/mL solution of CHCA (in 1:1 H_2O/ACN with 0.1% formic acid) on a 0.2 mm thick apple slice. The base peak in the mass spectrum is m/z 297 which corresponds to the nominal mass of the protonated molecule. The set of characteristic isotopic cluster peaks at m/z 297, 299, and 301 is consistent with the presence of two chlorine atoms. Peaks associated with the CHCA matrix are the dominant remaining peaks in the mass spectrum and do not interfere with the protonated imazalil peak. The limit of detection (LOD) for imazalil was evaluated by spiking imazalil standard with CHCA on an apple slice in the manner described above. Based on a value of 3 times the noise level of the blank, the LOD was determined to be 0.05 ppm.

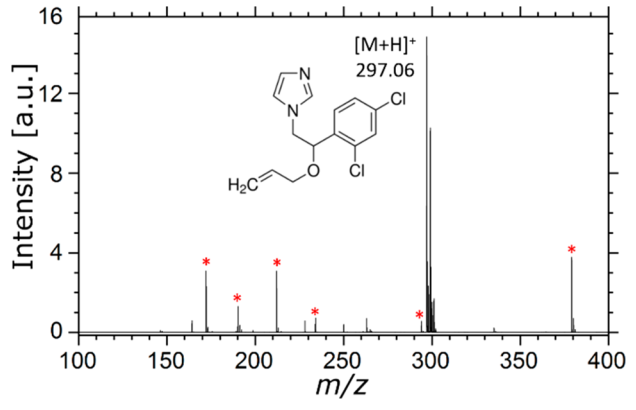

Figure 1. MALDI mass spectrum obtained from the application of 1 μL of a 1000 ppm imazalil (m/z 297.06 [M + H]$^+$) solution on an apple slice; matrix peaks are labeled with asterisks.

Figure 2 shows MALDI and optical images of sections of imazalil treated apples containing skin (top) and endocarp.

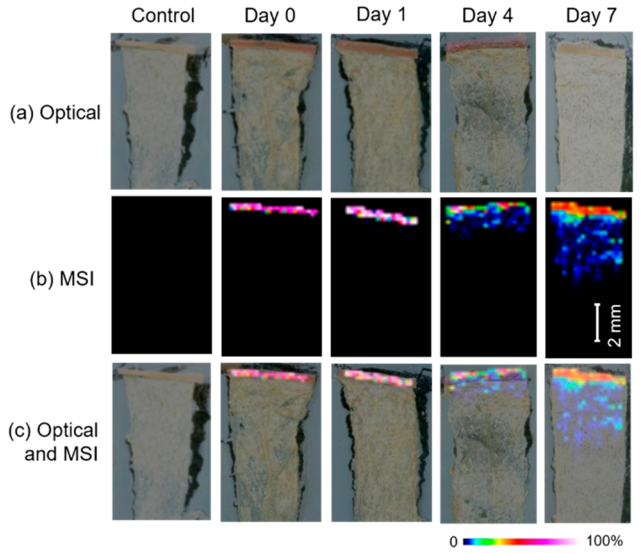

Figure 2. Penetration analysis of imazalil (m/z 297.06 [M + H]$^+$) in apples by MALDI imaging on Days 0, 1, 4, and 7 after dipping application of imazalil: (a) optical image of apple slices, (b) MALDI imaging of imazalil, and (c) merged optical and MALDI image.

These apples were treated with imazalil and stored for the indicated number of days. Figure 2a depicts the optical images of apple slices, Figure 2b shows the MALDI imaging of imazalil, and Figure 2c shows the merged optical and MALDI images. The heat map of Figure 2b was obtained by plotting the intensity of m/z 297.06 ± 0.2. The control section was treated as indicated above, and imazalil was not detected. On Day 0 (30 min after imazalil application), imazalil was detected in the skin and was not detected in the inner region. The same was found on Day 1, with the compound slightly more distributed. The images of apple sections 4 days after fungicide application showed that a small quantity of imazalil migrated approximately 1 mm toward the inner region, even though the largest quantity remained in the skin. On Day 7, the imaging results show the migration of imazalil approximately 3 mm inside the apple.

Of some concern is whether the vacuum drying step prior to matrix application and MALDI imaging modifies the thickness and size of apple sections which could affect the measurement accuracy of the imazalil diffusion depth. Drying is a necessary step to ensure adhesion of the apple slice to the microscope slide surface and prevent detachment of the section in the high-vacuum source of the MALDI mass spectrometer. In addition, it reduces the amount of water in the sample, which reduces analyte migration during matrix deposition. The vacuum drying may reduce the thickness, but a thin and dry section improves the ion signal in MALDI-MS analysis. The

DOI: 10.1021/acs.analchem.9b00566
Anal. Chem. 2019, 91, 6051−6056

area of the apple sections did not change measurably on drying.

Ambient laser ablation sampling and ESI-MS were used to measure the concentration of imazalil inside the apple. Areas of 0.2 mm × 1 mm were ablated from the skin and areas of 1 mm × 1 mm were ablated and collected from the skin toward the endocarp (Figure 3). Sampling was accomplished in a diagonal

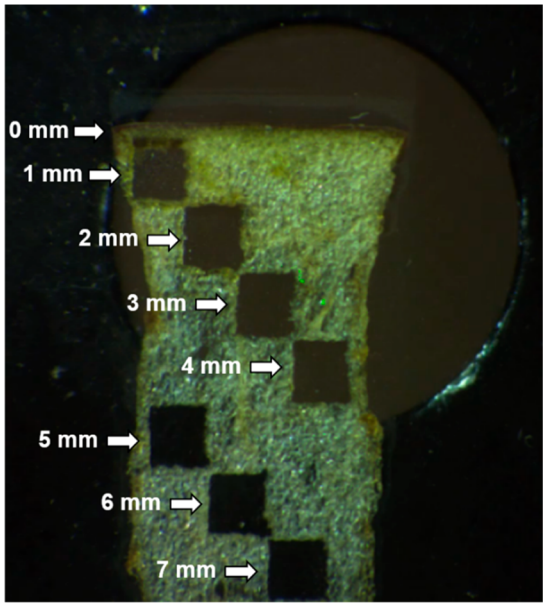

Figure 3. Apple regions (height 1 mm; width 1 mm; thickness 0.2 mm) ablated from the skin (0 mm) to the inner region (7 mm).

pattern to avoid cross-contamination, if any, from adjacent sampled regions. Additional experiments were performed to verify that the concentration of imazalil was constant across sections. Three regions of 1 mm^2 area in three different apples (three regions for each apple) were ablated in a horizontal pattern, captured, and analyzed by ESI-MS. The imazalil concentration was determined as constant at approximately 94%.

Before quantification, the overall extraction efficiency was evaluated (Table 1). The experiment was aimed at evaluating

Table 1. Overall Extraction Efficiency for Imazalil in Apples

concentration (ppm)	transfer efficiency (%)
0.005	62 ± 2
0.1	61 ± 3
1	62 ± 3

the total sampling efficiency of the approach, including laser ablation, capture, vortexing, centrifugation, extraction of the supernatant, drying under vacuum, and resuspension of sample in solvent for MS analysis. For this reason, a solution of imazalil in ACN was used as a control for comparison with laser ablation and ESI-MS sampling. Three different concentration imazalil solutions (in triplicate) were deposited on 1 mm^2 areas of three different apples. Each apple area was ablated, captured in 200 μL of ACN, vortexed, and centrifuged. The supernatant was dried and resuspended in 30 μL of ACN with 0.1% FA, and the resulting solution was injected into the ESI source. The peak intensity of m/z 297 $[M + H]^+$ was monitored. The control samples were solutions with the same concentrations as above. The transfer efficiency was determined from the ratio of the imazalil peak intensity from the recovered material to that from the control. The resulting efficiency of 60% is comparable to that obtained for sampling of biomolecules from animal tissue using this laser system.[54,55]

Localized quantification experiments were performed with sections of imazalil treated apples. The apple sections were ablated (as shown in Figure 3) and analyzed by ESI-MS. A representative positive ion ESI mass spectrum of imazalil $[M + H]^+$ from an apple section is shown in Figure 4. Sodium and potassium imazalil adduct ions were below the limit of detection of the instrument.

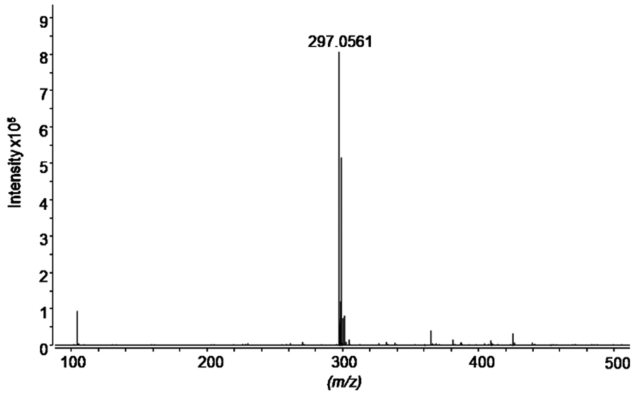

Figure 4. ESI(+) mass spectrum of imazalil (m/z 297.0561 $[M + H]^+$) after ablation of an apple section on Day 7.

The concentration of imazalil from the skin to the inner region of the apple is shown in Table 2. The limit of quantification (LOQ) was 0.005 ppm based on 10 times the signal-to-noise ratio. On Day 0, imazalil was found only in the skin (labeled as 0 mm in the table) at 2.4 ppm. On Day 1, a concentration of 0.024 ppm was detected in the first millimeter inside the apple. On Day 4, 0.015 ppm imazalil were found in the third millimeter inside the fruit. On Day 7, 0.015 ppm were detected in the sixth millimeter. No imazalil was found deeper than 6 mm . The concentration of imazalil in the first millimeter on Day 1, in the second and third millimeters on Day 4, and in the fourth to sixth millimeters on Day 7 are below the limit of detection of the MALDI method (0.05 ppm), and consequently imazalil was not detected in those regions during the imaging experiments.

From Table 2, it can be seen that the total concentration of imazalil on Day 7 is approximately 80% of that observed on Day 0, which corresponds to approximately 3% loss per day. To test whether this loss could be a result of photodegradation, an open microcentrifuge tube containing 1 ppm imazalil standard solution in ACN was exposed to a 4 W 254 nm UV lamp for 4 h at a distance of approximately 5 mm. An imazalil solution at 1 ppm which was not exposed to the UV lamp was used as a control. Both solutions were analyzed by ESI-MS, and the mass spectra are shown in Figure S-3. A possible photodegradation product of m/z 261.0795 ($[C_{14}H_{13}ClN_2O] + H^+$, loss of HCl from imazalil) was found, but a corresponding peak was not observed in the ESI mass spectra of imazalil in apple or in the mass spectra obtained for MALDI imaging. The mass spectra showed no significant differences in peak profile that could indicate photodegradation.

The rate and extent of transport of imazalil is consistent with previous studies. For example, the distribution of imazalil in

DOI: 10.1021/acs.analchem.9b00566
Anal. Chem. 2019, 91, 6051−6056

Table 2. Concentration of Imazalil from Skin (0 mm) to the Inner Region (7 mm) in Apple[a]

	concentration (ppm)			
distance from skin (mm)	Day 0	Day 1	Day 4	Day 7
0	2.425 ± 0.105	2.161 ± 0.053	1.748 ± 0.093	1.252 ± 0.026
1	BLQ	0.024 ± 0.003	0.199 ± 0.016	0.415 ± 0.051
2	BLQ	BLQ	0.019 ± 0.002	0.181 ± 0.020
3	BLQ	BLQ	0.015 ± 0.002	0.059 ± 0.003
4	BLQ	BLQ	BLQ	0.022 ± 0.009
5	BLQ	BLQ	BLQ	0.019 ± 0.009
6	BLQ	BLQ	BLQ	0.015 ± 0.008
7	BLQ	BLQ	BLQ	BLQ

[a]BLQ = below the limit of quantification

fruit after storage has been studied previously using gas and liquid chromatography. In a study of oranges using HPLC, it was found that 10−20% of the applied imazalil penetrated beyond the outer 1 mm of the fruit and into the interior of the fruit after 1 week.[6] The distribution of imazalil in lemons was probed by GC−MS and it was found that the migration into the interior was slow and that approximately 10% of the pesticide was present in the albedo with the remainder in the flavedo after 60 days.[59] Some indications of slow degradation of the fungicide over time with a 10−20 week half-life were observed. A study of the distribution of imazalil in apples quantified by HPLC showed that 70−90% of the pesticide was observed in the peel after 20 days.[60] Approximately 20−25% of the pesticide remained in the fruit after 155 days.

The results above are consistent with previous mass spectrometry imaging of fungicides. MALDI imaging has been used to study the penetration of the fungicide procymidone in cucumbers, and the results showed a fungicide diffusion from the skin to the inner region 1 day after its application.[7] The cucumbers were dissected by hand, and the fungicide was detected by GC−MS. No loss of the fungicide over time was observed. Laser ablation electrospray was used to map the distribution of imazalil in lemons and oranges and diphenylamine in apples.[61] Imaging was performed at 1 mm resolution, and the fungicide was observed primarily at the surface of the fruit.

CONCLUSION

A combination of MALDI imaging and IR laser ablation sampling followed by ESI-MS was used to localize and quantify the fungicide imazalil in apples after external application. MALDI imaging was used to visualize the penetration of the compound into the apple over time. Images of apple slices showed the penetration depth of imazalil up to 7 days. Ambient sampling using laser ablation and ESI-MS were used to quantify the imazalil residue within the apple. The fungicide was detected in the inner part of the apple 1 day after its application. The rate of penetration of detectable imazalil was approximately 1 mm per day. A decline in imazalil concentration in the apple skin was detected over the course of the 7 days. Seven days after application of the fungicide, a concentration of 0.015 ppm was found 6 mm inside the apple. The overall extraction efficiency was approximately 60%.

MALDI imaging was useful for the visualization of fungicide penetration in apples, but the high limit of detection did not allow verification of deeper penetration. Laser ablation with ESI-MS provided the detection of the fungicide in low concentrations, allowing the determination of the fungicide deeper than MALDI imaging results. In addition, laser ablation allowed efficient homogenization, which enabled extractions within seconds. At the same time, the preliminary screening with MALDI allowed us to determine the sampling size of the areas for laser ablation and capture as well as the number and the position of the locations. Future work is aimed at using the same section for MALDI imaging and then laser ablation, which is expected to avoid any potential bias derived from the use of consecutive sections to reduce sample preparation steps and speed up the analysis.

ASSOCIATED CONTENT

Supporting Information

The Supporting Information is available free of charge on the ACS Publications website at DOI: 10.1021/acs.analchem.9b00566.

Imazalil structure and physicochemical properties; calibration curve obtained from ESI-MS analysis; and mass spectra from photodegradation experiment (PDF)

AUTHOR INFORMATION

Corresponding Authors

*E-mail: kkmurray@lsu.edu.
*E-mail: boniek@ufg.br.

ORCID

Igor Pereira: 0000-0002-4329-0701

Author Contributions

All authors have given approval to the final version of the manuscript.

Notes

The authors declare no competing financial interest.

ACKNOWLEDGMENTS

This material is based upon work supported by the National Science Foundation under Grant No. CHE-1709526. I.P. gratefully acknowledges support from the Brazilian Federal Agency for Support and Evaluation of Graduate Education (CAPES) under PDSE Program-88881.132855/2016-01.

REFERENCES

(1) Matthews, G. *Pesticides: Health, Safety and the Environment*, 2nd ed.; John Wiley & Sons: Hoboken, NJ, 2016.
(2) Kim, K.-H.; Kabir, E.; Jahan, S. A. *Sci. Total Environ.* **2017**, *575*, 525−535.
(3) Mostafalou, S.; Abdollahi, M. *Arch. Toxicol.* **2017**, *91*, 549−599.
(4) Hernández, A. F.; Tsatsakis, A. M. *Food Chem. Toxicol.* **2017**, *103*, 188−193.
(5) Bajwa, U.; Sandhu, K. S. *J. Food Sci. Technol.* **2014**, *51*, 201−220.
(6) Brown, G. E.; Dezman, D. J. *Plant Dis.* **1990**, *74*, 927−930.

DOI: 10.1021/acs.analchem.9b00566
Anal. Chem. 2019, 91, 6051−6056

(7) Taira, S.; Tokai, M.; Kaneko, D.; Katano, H.; Kawamura-Konishi, Y. *J. Agric. Food Chem.* **2015**, *63*, 6109−6112.
(8) Mostafalou, S.; Abdollahi, M. *Arch. Toxicol.* **2017**, *91*, 549−599.
(9) Schirra, M.; D'aquino, S.; Cabras, P.; Angioni, A. *J. Agric. Food Chem.* **2011**, *59*, 8531−8542.
(10) D'Aquino, S.; Schirra, M.; Palma, A.; Angioni, A.; Cabras, P.; Migheli, Q. *J. Agric. Food Chem.* **2006**, *54*, 4721−4726.
(11) Barkai-Golan, R. *Postharvest Diseases of Fruits and Vegetables. Development and Control*, 1st ed.; Elsevier Science B.V.: Amsterdam, The Netherlands, 2001.
(12) Erasmus, A.; Lennox, C. L.; Korsten, L.; Lesar, K.; Fourie, P. H. *Postharvest Biol. Technol.* **2015**, *107*, 66−76.
(13) Jeong, R.-D.; Chu, E.-H.; Shin, E.-J.; Lee, E.-S.; Kwak, Y.-S.; Park, H.-J. *Lett. Appl. Microbiol.* **2015**, *61*, 437−445.
(14) Cabras, P.; Schirra, M.; Pirisi, F. M.; Garau, V. L.; Angioni, A. *J. Agric. Food Chem.* **1999**, *47*, 3352−3354.
(15) Altieri, G.; Di Renzo, G. C.; Genovese, F.; Calandra, M.; Strano, M. C. *Biosyst. Eng.* **2013**, *115*, 434−443.
(16) Kellerman, M.; Joubert, J.; Erasmus, A.; Fourie, P. H. *Postharvest Biol. Technol.* **2016**, *121*, 159−164.
(17) Tanaka, T. *Reprod. Toxicol.* **1995**, *9*, 281−288.
(18) Şişman, T.; Türkez, H. *Toxicol. Ind. Health* **2010**, *26*, 641−648.
(19) Kruve, A.; Lamos, A.; Kirillova, J.; Herodes, K. *Proc. Estonian Acad. Sci. Chem.* **2007**, *56*, 134−141.
(20) Sharma, D.; Nagpal, A.; Pakade, Y. B.; Katnoria, J. K. *Talanta* **2010**, *82*, 1077−1089.
(21) Alder, L.; Greulich, K.; Kempe, G.; Vieth, B. *Mass Spectrom. Rev.* **2006**, *25*, 838−865.
(22) Grimalt, S.; Dehouck, P. *J. Chromatogr. A* **2016**, *1433*, 1−23.
(23) Uclés, S.; Uclés, A.; Lozano, A.; Martínez Bueno, M. J.; Fernández-Alba, A. R. *J. Chromatogr. A* **2017**, *1501*, 107−116.
(24) Picó, Y.; Font, G.; Moltó, J. C.; Mañes, J. *J. Chromatogr. A* **2000**, *882*, 153−173.
(25) Niessen, W. M. A.; Manini, P.; Andreoli, R. *Mass Spectrom. Rev.* **2006**, *25*, 881−899.
(26) Stachniuk, A.; Fornal, E. *Food Anal. Method.* **2016**, *9*, 1654−1665.
(27) Masiá, A.; Suarez-Varela, M. M.; Llopis-Gonzalez, A.; Picó, Y. *Anal. Chim. Acta* **2016**, *936*, 40−61.
(28) Lagarrigue, M.; Caprioli, R. M.; Pineau, C. *J. Proteomics* **2016**, *144*, 133−139.
(29) Spengler, B. *Anal. Chem.* **2015**, *87*, 64−82.
(30) Gessel, M. M.; Norris, J. L.; Caprioli, R. M. *J. Proteomics* **2014**, *107*, 71−82.
(31) Ellis, S. R.; Bruinen, A. L.; Heeren, R. M. A. *Anal. Bioanal. Chem.* **2014**, *406*, 1275−1289.
(32) Norris, J. L.; Caprioli, R. M. *Chem. Rev.* **2013**, *113*, 2309−2342.
(33) Kaspar, S.; Peukert, M.; Svatos, A.; Matros, A.; Mock, H. P. *Proteomics* **2011**, *11*, 1840−1850.
(34) Boughton, B. A.; Thinagaran, D.; Sarabia, D.; Bacic, A.; Roessner, U. *Phytochem. Rev.* **2016**, *15*, 445−488.
(35) Sturtevant, D.; Lee, Y. J.; Chapman, K. D. *Curr. Opin. Biotechnol.* **2016**, *37*, 53−60.
(36) Kadam, S. U.; Misra, N. N.; Zaima, N. *RSC Adv.* **2016**, *6*, 33537−33546.
(37) Annangudi, S. P.; Myung, K.; Adame, C. A.; Gilbert, J. R. *Environ. Sci. Technol.* **2015**, *49*, 5579−5583.
(38) Anderson, D. M. G.; Carolan, V. A.; Crosland, S.; Sharples, K. R.; Clench, M. R. *Rapid Commun. Mass Spectrom.* **2010**, *24*, 3309−3319.
(39) Mullen, A. K.; Clench, M. R.; Crosland, S.; Sharples, K. R. *Rapid Commun. Mass Spectrom.* **2005**, *19*, 2507−2516.
(40) Bartels, B.; Svatoš, A. *Front. Plant Sci.* **2015**, *6*, 1−7.
(41) Wu, C.; Dill, A. L.; Eberlin, L. S.; Cooks, R. G.; Ifa, D. R. *Mass Spectrom. Rev.* **2013**, *32*, 218−243.
(42) Cheng, S.-C.; Shiea, C.; Huang, Y.-L.; Wang, C.-H.; Cho, Y.-T.; Shiea, J. *Anal. Methods* **2017**, *9*, 4924−4935.
(43) Shrestha, B.; Vertes, A. *Anal. Chem.* **2009**, *81*, 8265−8271.
(44) Brauer, J. I.; Beech, I. B.; Sunner, J. *J. Am. Soc. Mass Spectrom.* **2015**, *26*, 1538−1547.
(45) Fang, J.; Schneider, B. *Phytochem. Anal.* **2014**, *25*, 307−313.
(46) Happyana, N.; Agnolet, S.; Muntendam, R.; Dam, A. V.; Schneider, B. *Phytochemistry* **2013**, *87*, 51−59.
(47) Yi, L.; Liang, Z.-T.; Peng, Y.; Yao, X.; Chen, H.-B.; Zhao, Z.-Z. *J. Chromatogr. A* **2012**, *1248*, 93−103.
(48) Park, S.-G.; Murray, K. K. *J. Mass Spectrom.* **2012**, *47*, 1322−1326.
(49) Park, S.-G.; Murray, K. K. *J. Am. Soc. Mass Spectrom.* **2011**, *22*, 1352−1362.
(50) Park, S.-G.; Murray, K. K. *Rapid Commun. Mass Spectrom.* **2013**, *27*, 1673−1680.
(51) Ovchinnikova, O. S.; Kertesz, V.; Van Berkel, G. J. *Anal. Chem.* **2011**, *83*, 1874−1878.
(52) Ren, L.; Robertson, W. D.; Reimer, R.; Heinze, C.; Schneider, C.; Eggert, D.; Truschow, P.; Hansen, N.-O.; Kroetz, P.; Zou, J.; Miller, R. J. D. *Nanotechnology* **2015**, *26*, 284001.
(53) Pettit, M. E.; Donnarumma, F.; Murray, K. K.; Solouki, T. *Anal. Chim. Acta* **2018**, *1034*, 102−109.
(54) Wang, K.; Donnarumma, F.; Baldone, M. D.; Murray, K. K. *Anal. Chim. Acta* **2018**, *1027*, 41−46.
(55) Wang, K.; Donnarumma, F.; Herke, S. W.; Herke, P. F.; Murray, K. K. *Anal. Bioanal. Chem.* **2017**, *409*, 4119−4126.
(56) Barrett, D. M.; Lee, C. Y.; Liu, F. W. *J. Food Biochem.* **1991**, *15*, 185−199.
(57) Johnson, D. S.; Colgan, R. J. *Postharvest Biol. Technol.* **2003**, *27*, 59−68.
(58) Donnarumma, F.; Cao, F.; Murray, K. K. *J. Am. Soc. Mass Spectrom.* **2016**, *27*, 108−116.
(59) Dore, A.; Molinu, M. G.; Venditti, T.; D'Hallewin, G. *J. Agric. Food Chem.* **2009**, *57*, 623−631.
(60) Cano, M. P.; la Plaza, J. L. D.; Muñoz-Delgado, L. *Pestic. Sci.* **1987**, *19*, 283−287.
(61) Nielen, M. W. F.; van Beek, T. A. *Anal. Bioanal. Chem.* **2014**, *406*, 6805−6815.

DOI: 10.1021/acs.analchem.9b00566
Anal. Chem. 2019, 91, 6051−6056